Characterizing the effect of environmental variability on local vibrations experiences on the Haringvlietbrug

Kortendijk, C.N.; Besseling, Floris; Jolink, Chris; Lourens, E.

Publication date
2021

Document Version
Accepted author manuscript

Citation (APA)
Kortendijk, C. N., Besseling, F., Jolink, C., & Lourens, E. (2021). *Characterizing the effect of environmental variability on local vibrations: experiences on the Haringvlietbrug*. Paper presented at 10th International Conference on Structural Health Monitoring of Intelligent Infrastructure, Porto, Portugal.

Characterizing the effect of environmental variability on local vibrations: experiences on the Haringvlietbrug

C.N. Kortendijk[1,2], F. Besseling[2], C. Jolink[2], E. Lourens[1]
[1]Department of Engineering Structures, Faculty of Civil Engineering and GeoSciences, Delft University of Technology, Stevinweg 1, 2628CN Delft, Netherlands
[2]Witteveen+Bos Consulting Engineers, Leeuwenbrug 8, 7411TJ Deventer, The Netherlands
email: coen.kortendijk@witteveenbos.com, floris.besseling@witteveenbos.com, chris.jolink@witteveenbos.com, e.lourens@tudelft.nl

ABSTRACT: When employing vibration-based damage detection methods for monitoring the structural health of bridges, it is often possible to increase damage feature sensitivity by focusing on local as opposed to global vibrations. This heightened sensitivity, however, comes at a cost: by moving towards the higher frequency ranges and more local behavior, the effects of environmental variability become increasingly pronounced. In an attempt to characterize and quantify the effect of specifically temperature variations on the local vibrations, an extensive long-term monitoring campaign was performed on the Haringvlietbrug, a steel box-girder bridge in the Netherlands. Temperatures were measured on various components of the bridge, including the top and bottom of the asphalt layers. It was found that complex temperature gradients are formed especially in situations where the radiation from the sun strikes the bridge at oblique angles. More importantly, the temperature variations in the asphalt layers were found to strongly impact the natural vibration properties of the bridge in the targeted high-frequency ranges. The obtained results provide valuable indications as to the environmental parameters to monitor when designing vibration-based structural health monitoring systems for local damage detection in bridges.

KEY WORDS: Environmental variability, temperature effects, influence of asphalt, local vibrations, steel bridge.

1 INTRODUCTION

One of the main challenges in bringing vibration-based SHM systems for civil infrastructures to maturity, is effectively handling the effect of environmental variability on the features used for damage detection. This so-called data normalization problem [1], can roughly speaking be attempted in two ways [2]. The first strategy is to directly measure the changing environmental parameters. When direct measurements of the changing environment are not available, one can attempt to define a normal condition by measuring for long periods of time on an undamaged structure. One obvious disadvantage of this approach is the fact that novelties in the structural behaviour can only be detected insofar as they occur within environments that have already existed within the timeframe of the monitoring campaign. Another, more important disadvantage, is that when a normal condition encompassing huge variations of impactful environmental parameters is defined, any traceable sensitivity to damage may be lost. To ensure traceability, especially for small or initial damages, it is therefore often necessary to additionally measure the relevant environmental conditions. If comprehensive measurements of these conditions are available, the data normalization problem can be solved using for instance regression techniques [3].

One of the key questions then remaining, is which environmental parameters are *relevant*. This depends on the structure, the type of damage to be detected, and how the damage features are derived from the measurements. In this contribution, the focus is on a steel box-girder bridge, the detection of fatigue cracks between transverse beams and longitudinal stiffeners, and damage features that are derived from high-frequency (>50Hz) vibrations. Given these application-specific boundary conditions, an assessment of the impact of temperature variations on the local vibration behaviour of parts of the deck plate is made. Long term vibration and temperature measurements are performed and the measurement data are evaluated. Some interesting observations regarding the complexity of the measured temperature gradients are presented in this paper.

Temperature effects in steel bridges are not limited only to the steel structure itself. Also asphalt layers overlaying the steel structure are affected. Asphalt temperatures typically vary over an even wider range, compared to steel temperatures. For asphalt, temperature effects are not limited to temperature induced stress, but also the physical material properties of asphalt are clearly a function of temperature. To relate measured asphalt temperatures to changes in stiffness and dynamic properties, asphalt material test results are used to perform asphalt material modelling. The purpose of this modelling is to construct asphalt material behaviour curves, which cover the temperature and frequency ranges for the Haringvlietbrug. Using the measured temperature data and the asphalt models an assessment of specific subsystems is made, analysing the effect of the measured temperatures on local vibrations. It is shown that the fundamental natural frequency of some of the analysed subsystems might change with as much as 47 percent due to variations in asphalt temperatures alone. A verification of the hypotheses from the theoretical models is ongoing. The results presented in this contribution provide valuable indications as to the environmental parameters to monitor when designing vibration-based structural health monitoring systems for local damage detection in bridges.

2 HARINGVLIETBRUG MEASUREMENT CAMPAIGN

The Haringvlietbrug is a continuous steel box girder bridge built in the 1960's and consisting of 10 spans of 106 m each. The bridge is oriented in the north-south direction (heading of 21° North), and contains 2x2 highway lanes, with a smaller side-road on the east side. A typical cross-section is shown in Figure 1. The 10 mm steel deck plate is supported by longitudinal stiffeners distributed 0.3 m centre-to-centre (c.t.c.), and spanning between transfer frames placed at 2.2 m c.t.c. Every 4th transfer frame contains struts, supporting the cantilever. The deck surfacing consists of a 30 mm ZOAB[1] layer on top of a 30 mm layer of guss-asphalt, separated by waterproofing membranes.

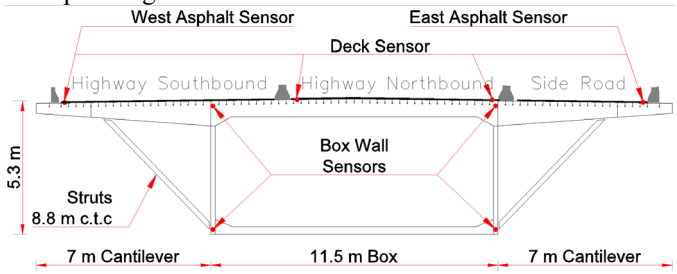

Figure 1. Cross-section of the bridge

Asphalt temperatures are measured using PT1000 temperature sensors positioned at the West and East side of the bridge, at 10 and 54 mm from the top and 150 mm from the edge of the asphalt surface, see Figure 2. Sensors are also placed at the bottom of the deck plate, below the asphalt sensors. The temperature of the box walls is measured using FBG temperature sensors at 200 mm from the top and bottom, respectively.

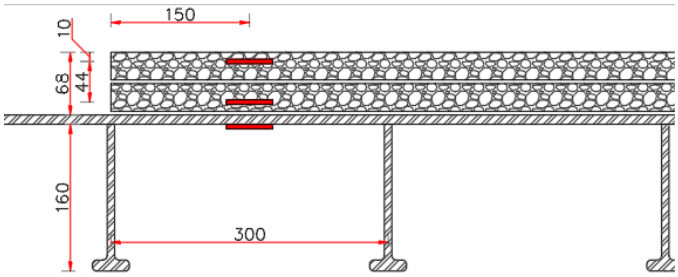

Figure 2. Asphalt and deck plate sensor position

All temperature sensors are sampled at least once every 5 minutes starting May 20, 2020. From this dataset a period of 3 relatively warm days between May 30, 2020, and June 01, 2020, is shown in Figure 3 and Figure 4.

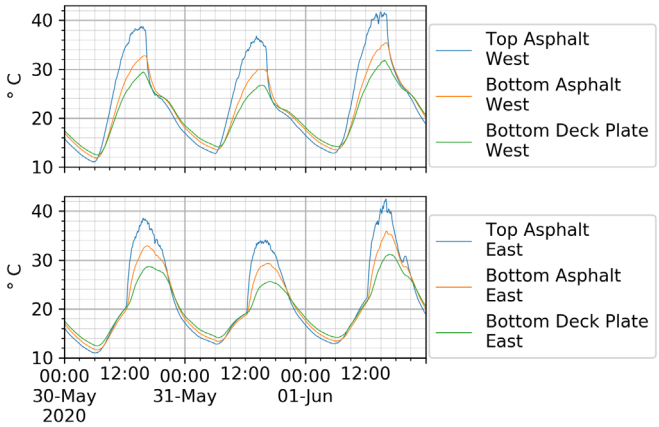

Figure 3. Measured cantilever deck temperatures

The top asphalt layer reaches temperatures of up to 40 °C, and the bottom asphalt layer reaches temperatures of up to 35 °C, as shown in Figure 3. The West and East temperatures show a distinctively different daily pattern which will be elaborated on in section 3.1.

The bottom temperature sensor of the box wall also shows distinct temperature spikes in the morning and evening for the East and West box walls, respectively (c.f. Figure 4). These will be further discussed in section 3.2.

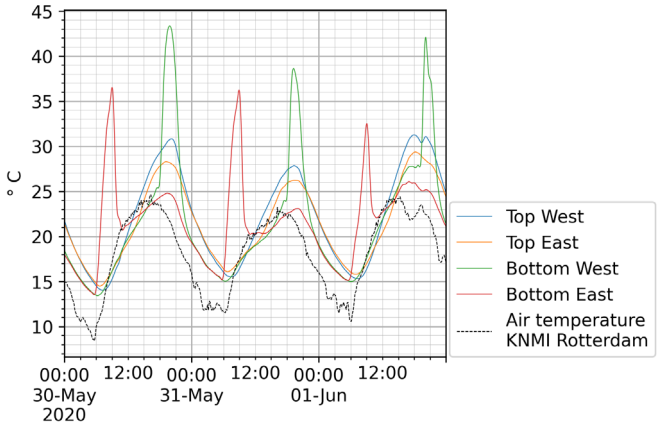

Figure 4. Measured box wall temperatures

3 COMPLEXITY OF MEASURED TEMPERATURE GRADIENTS

The long term temperature monitoring of the Haringvlietbrug is still ongoing. However, even in the short period shown, some distinct patterns are found, namely the influence of shade on the deck and the box walls, and the behaviour of hollow sections.

[1] ZOAB is a Dutch mixture similar to porous asphalt concrete.

3.1 Shade on deck.

The daily pattern for the deck temperatures in Figure 3 shows two distinct transitions.

- In the morning, the west-side asphalt temperatures show a smooth increase from 12 ºC at 06:00, to over 30 ºC, while the east-side temperatures stay below 20 ºC until noon, after which a steep upward gradient is observed.
- At approximately 16:00, the west-side temperature sensors show a sudden drop, that does not occur for the east-side sensors.

The traffic lanes of the Haringvlietbrug are separated by steel barriers as can be seen in Figure 1. The temperature sensors are placed 150 mm from the edge of the asphalt, and thus very close to these barriers. Using Figure 5, the cause of these patterns may be found in barrier induced shade.

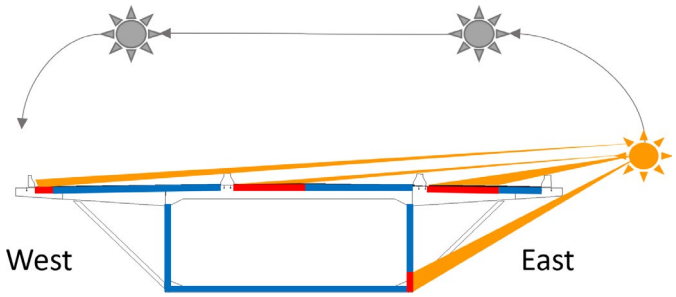

Figure 5 Solar radiation in the morning

To verify that shade causes these transitions, an analytical 1D heat flow analysis of the deck, including longitudinal stiffeners, was performed using the bridge geometry, the solar inclination [9], solar intensity[10], and the ambient temperature [10]. For the top asphalt temperature sensor on the west side, the result is shown in Figure 6. The onset of shade is calculated from solar data and measured geometry only. The model shows a good fit for both the temperature as the onset of the temperature drop, implying the onset of the temperature drop is caused by shade and the temperature gradients are clearly dominated by direct sun radiation impact. A similar analysis was performed for the East side further confirming these conclusions.

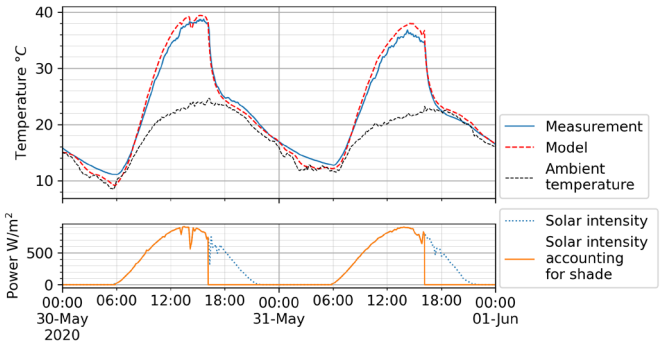

Figure 6 Heat flow results for the top East asphalt temperature

The size and position of the shade from the barrier changes throughout the day, as shown in Figure 7. This implies that throughout the day the absolute temperatures as well as the temperature gradients are non-constant over the bridge deck structure.

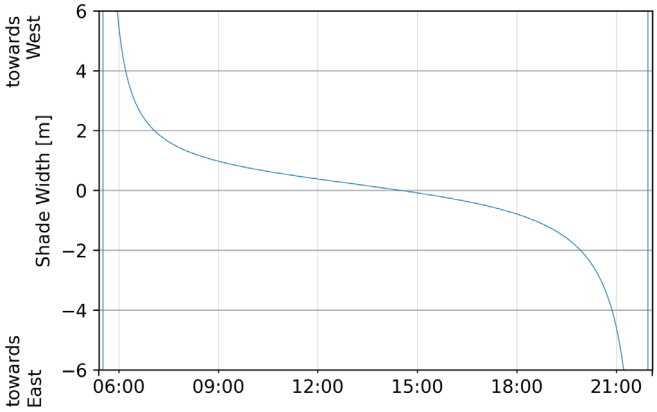

Figure 7 Shade-width caused by a 0.6 m high barrier

3.2 Box wall temperature gradients

The temperatures of the box walls are shown in Figure 4. Here large spikes are clearly visible for the bottom sensors. These spikes may also be explained by a low sun inclination directly affecting the wall underneath the cantilever as illustrated in Figure 5.

The temperature of the bottom East wall rises early in the morning, and suddenly drops after 09:00. The cantilever is approximately 7 m wide, and the bottom box wall sensor is approximately 4.7 m below the cantilever edge. A solar inclination below 34º would therefore allow direct sunlight on the lower part of the box wall. Figure 8 shows the solar inclination is below 34º until 09:30, confirming the onset of the temperature drop on the lower East box wall is triggered by shade. In the evening the inclination drops below 34 at 18:00, perfectly coinciding with the onset of the temperature spike at the West bottom box wall.

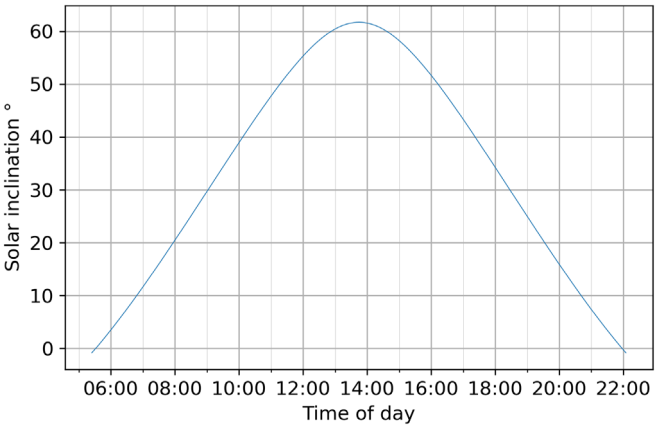

Figure 8 Solar inclination

3.3 *Air temperature inside hollow sections.*

Figure 9 shows measurements of deck plate temperatures at the cantilever and above the box. Measurements indicate that the deck above the box reaches higher temperatures than the cantilever deck, and this temperature difference remains throughout the night, even though the construction is similar. However, both the top ánd bottom sides of the cantilever deck are exposed to environmental influences such as the ambient air temperature and wind, while the bottom of the deck above the box is shielded from the environment.

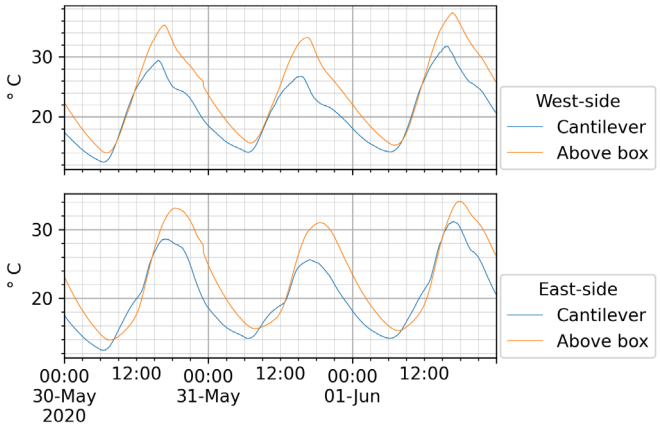

Figure 9 Deck plate temperatures

To further investigate this influence, an air temperature sensor was placed inside the box. Figure 10 shows that on cool days the temperature inside the box is similar to that of the KNMI weather station, while on warm days a significant temperature rise occurs, and the air maintains a temperature higher than the ambient air throughout the night.

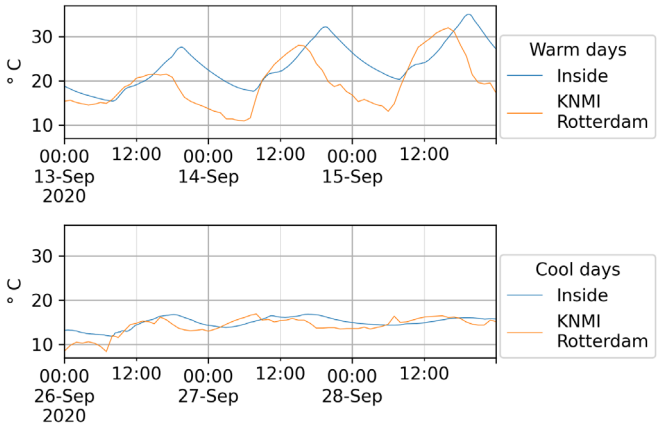

Figure 10 Air temperature

The same 1D heat flow model as was used in section 3.1, is used to model the temperature of the deck plate above the box. The top graph in Figure 11 shows the results, assuming the air temperature inside the box is identical to the outside air temperature. The centre graph in Figure 11 shows that including the measurement of the air temperature inside the box, significantly improves the results.

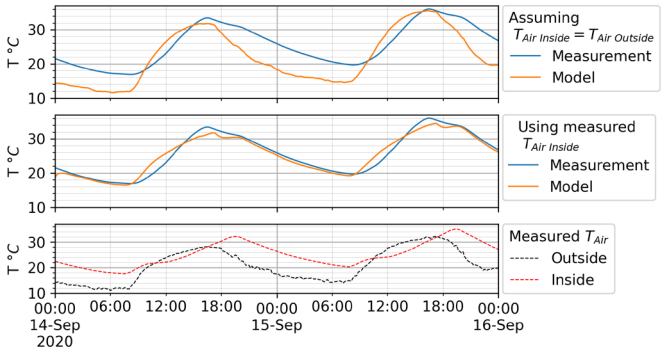

Figure 11 Heat flow results for deck plate above the box

3.4 *Limitations due to complexity of gradients*

The design of the measurement setup was subject to practical limitations and new insights regarding the complexity of these temperature gradients was obtained from the Haringvlietbrug project. Design codes and standards do not address such complex temperature gradients in detail [6,7,8]. Therefore, the measurement setup did not account for the complexity of the aforementioned gradients, preventing a detailed investigation into the exact shape of these shade-induced temperature gradients. This induces uncertainty regarding the temperature induced stress distribution in the cross section. Preliminary analyses using a 3D FE-model of the bridge containing 11 linear temperature gradient load cases, serving as interpolation functions, has shown that especially the box wall temperature gradient requires further investigation. Verification of these theoretical models is ongoing and requires a modified measurement setup.

However, uncertainty due to temperature-induced stress may be reduced by focusing on periods containing the smallest gradients. In Figure 12, the blue graph shows the difference between the highest and lowest measured temperature, while the orange graph shows the solar radiation as obtained from KNMI. Two things can be noted. Firstly, the largest temperature differences are due to the lower parts of the box wall as discussed in section 3.2, and they don't occur at 14:00 when solar radiation peaks. And secondly, the smallest temperature difference occurs just before sunrise at 06:00. If this short period contains enough observations with adequate excitation for SHM, then the requirements for capturing these gradients may be relaxed. If measurement data of other periods is required, then this short period can be used as a reference point for calibrating the equipment and model.

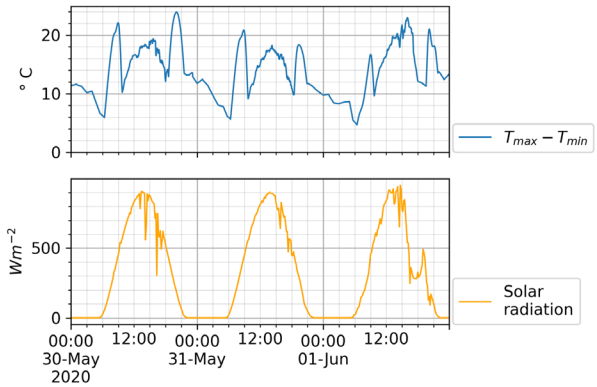

Figure 12 Gradient amplitude versus Solar radiation

4 ASPHALT MATERIAL MODELLING

The steel deck plate is covered with a multilayer asphalt system, with a composition as shown in Table 1. Asphalt has multiple temperature-dependent properties, among which Young's modulus, viscosity, the coefficients of thermal expansion & -contraction and Poisson's ratio. This study is limited to variations in effective Young's modulus, under the assumption that this is the parameter that has the most significant influence on deck plate vibration frequencies.

Table 1 Deck Composition

Layer [-]	**Material** [-]	**Thickness** [mm]	**Density** [kg/m^3]
1	ZOAB	30	2000
2	Parafor Ponts	4	1500
3	Guss Asphalt	30	2360
4	Mistral C	4	1500
5	Steel plate	10	7850

4.1 Supplied asphalt properties

Temperature- and frequency-dependent asphalt Young's modulus from laboratory tests are shown in Table 2 and Table 3. No specifications of the waterproofing membranes are available. The supplied asphalt parameters are valid for temperatures up to 20 °C, and loading frequencies between 5.86 and 58.59 Hz. This range does neither cover the measured temperatures of up to 40 °C for ZOAB and 35 °C for Guss asphalt nor the frequency range of interest, so material modelling is required to obtain an equivalent stiffness for those temperatures and frequencies. The procedure will be shown here for Guss asphalt, but is also applicable to ZOAB.

Table 2 Guss asphalt Young's modulus

[Hz]	**-10°C** [MPa]	**-05°C** [MPa]	**00°C** [MPa]	**5°C** [MPa]	**10°C** [MPa]	**15°C** [MPa]	**20°C** [MPa]
5.86	21213	17551	14207	11107	7962	5711	3745
9.77	21929	18357	15000	12023	8787	6421	4312
19.53	22842	19419	16198	13307	9992	7511	5185
25.39	23154	19792	16767	13790	10440	7922	5535
29.30	23317	19985	17037	14045	10689	8154	5732
35.16	23523	20230	17336	14378	11000	8447	5988
39.06	23621	20369	17520	14558	11180	8607	6130
50.78	23878	20658	17895	15020	11608	8995	6508
58.59	24000	20802	18119	15244	11812	9110	6683

Table 3 ZOAB Young's modulus

[Hz]	**-10°C** [MPa]	**-05°C** [MPa]	**00°C** [MPa]	**5°C** [MPa]	**10°C** [MPa]	**15°C** [MPa]	**20°C** [MPa]
5.86	21213	17551	14207	11107	7962	5711	3745
9.77	21929	18357	15000	12023	8787	6421	4312
19.53	22842	19419	16198	13307	9992	7511	5185
25.39	23154	19792	16767	13790	10440	7922	5535
29.30	23317	19985	17037	14045	10689	8154	5732
35.16	23523	20230	17336	14378	11000	8447	5988
39.06	23621	20369	17520	14558	11180	8607	6130
50.78	23878	20658	17895	15020	11608	8995	6508
58.59	24000	20802	18119	15244	11812	9110	6683

4.2 Construction of asphalt master curves

A plot of the supplied parameters for Guss asphalt is shown in Figure 13. Using the Time Temperature Superposition Principle (TTSP) [4,11] the results for each test temperature are shifted along the frequency axis until they align continuously using equation 1, and resulting in Figure 14. The measured curve for 15 °C is not shifted and is now called the reference temperature. The x-axis is relabelled to "reduced frequency", to indicate it includes the temperature dependence[11]. The obtained values for α_T are given in Table 4.

$$f_{\text{reduced}} = 10^{\log(f_{\text{test}})+\log(\alpha_T)} \quad (1)$$

Table 4 Shift factors for Guss asphalt

T [°C]	-10	-5	0	5	10	15	20
α_T [-]	4.10	3.02	2.18	1.45	0.65	0	-0.70

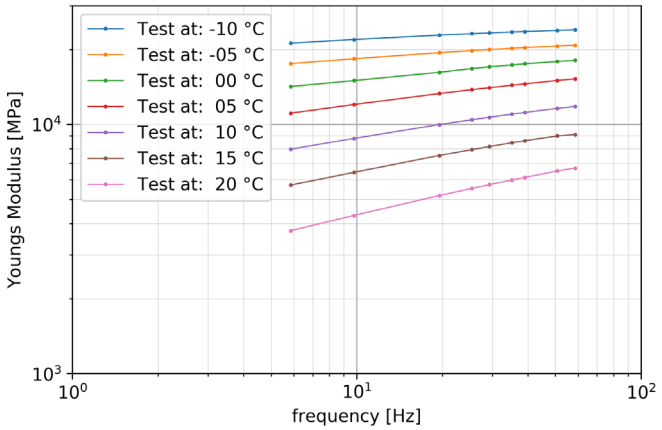

Figure 13 Supplied parameters guss asphalt

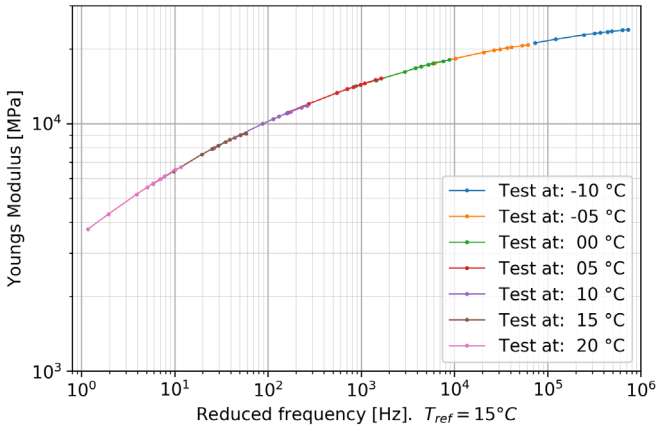

Figure 14 Guss asphalt master curve

The frequency-dependent asphalt stiffness may be described with a sigmoid function [11]. This function is fitted through the points in Figure 14 using a least squares algorithm (RMS error <61 MPa) resulting in equation (2):

$$\log\left(E_{\text{guss}}\right) = 1.13 + \frac{3.35}{1 + e^{-0.42\,(\log(f)+2.27)}} \quad \#(2)$$

$$\log(\alpha_t) = \frac{-16.04(T-15)}{124 + T - 15} \quad (3)$$

Finally, using a curve fit on the Williams-Landel-Ferry (WLF) equation [5] and the previously obtained shift factors from Table 4, shift factors can be predicted for other temperatures, as shown in equation (3) and Figure 15. The resulting temperature- and frequency-dependent asphalt stiffness is shown in Figure 16.

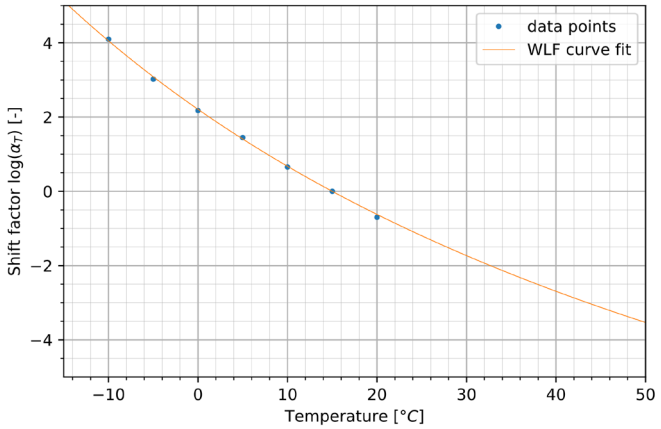

Figure 15 WLF curve

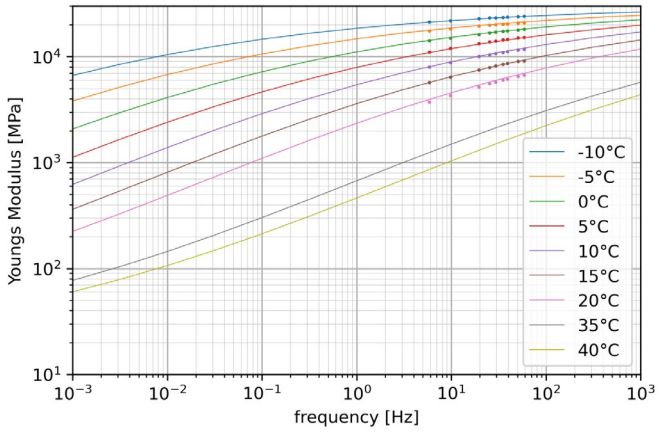

Figure 16 Modelled guss asphalt properties

5 LOCAL SUBSYSTEMS FOR FATIGUE CRACK DETECTION

For the detection of fatigue cracks between transverse beams and longitudinal stiffeners, local modes of the deck and stiffeners are of interest. The influence of asphalt on the frequency of these modes may be examined using discrete subsystems. Three subsystems of different sizes were modelled. The first and smallest scale subsystem comprises a 0.3x0.1 m section of deck plate including asphalt spanning two longitudinal stiffeners in the transverse direction. The second sub system contains a single 2.2 m span of the longitudinal stiffener including a section of deck plate and asphalt. The third and largest system considered is a 106 m bridge span.

5.1 Analytical approach to subsystem dynamics

The objective of the subsystem modelling is to examine the relative change of eigenfrequency due to asphalt temperature change. Using equation 5, the eigenfrequencies of the subsystems are assumed to be a function of composite member stiffness. Focusing on the relative effect, implies that the exact eigenfrequency is of no importance and subsystem boundary conditions do not affect the relative effect of changing asphalt stiffness. This assumption needs validation, but if proven correct it lowers the importance of understanding the exact complex boundary conditions of subsystems which are subject to significant uncertainty.

All of the subsystems may, under this assumption, be modelled as Euler-Bernoulli beams, supported with a pin on one end, and a pin-roller at the other end. Rigid bonds between the layers are assumed. Slip or shear that might exist due to the flexible membranes is ignored, resulting in upper-bound composite stiffnesses. Calculated values should only be evaluated relative to each other, and not as reliable absolute values.

Composite stiffness EI, and a first eigenfrequency f_1 are calculated using equations 4 and 5.

$$\text{EI} = \int_A E(z) z^2 \, dA \quad (4)$$

$$f_1 = \sqrt{\frac{\pi^4 \text{EI}}{\rho A l^4}} \cdot \frac{1}{2\pi} = \sqrt{EI}\sqrt{\frac{\pi^2}{4\rho A l^4}} \quad (5)$$

6 INFLUENCE OF TEMPERATURE ON LOCAL VIBRATIONS

Based on the measurements the asphalt is assumed to have a temperature of 15 ºC at night, while during the day the ZOAB- and guss asphalt reaches temperatures of 40 ºC and 35 ºC, respectively. For each of the subsystems and each of these temperatures the material properties, effective stiffness EI and first eigenfrequencies are calculated and subjected to a comparative evaluation. Verification of the predicted temperature effects against vibration measurement data is not presented here as it is part of ongoing research.

6.1 Sub system 1: Deck plate with asphalt.

The first sub system is a 100 mm wide strip of deck plate with asphalt, spanning 300 mm between two stiffeners, as shown in Figure 17.

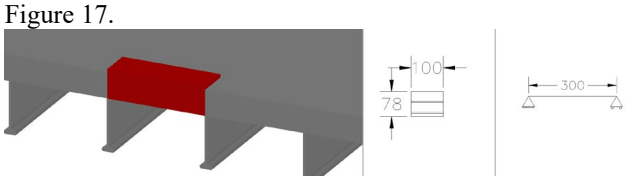

Figure 17 Deck plate subsystem

At night the temperature is approximately 15 ºC, and the first eigenfrequency at this temperature is shown in the first row of Table 5 as 1019 Hz. During the day the temperature rises to 40 ºC for the ZOAB-asphalt, and 35 ºC for the guss-asphalt layer. At these temperatures the asphalt stiffness is lower, resulting in a lower EI of the composite beam. The eigenfrequency is calculated to reduce to 582 Hz as shown in row 2. Assuming the eigenfrequency equals the loading-frequency, the asphalt stiffness is recalculated for this lower loading-frequency, as shown in row 3. The resulting calculated eigenfrequency drop is from 1019 to 538 Hz, a reduction of 47%.

Table 5 Deck plate subsystem

Input	E_{zoab} GPa	E_{guss} GPa	EI Nm^2	f_1 Hz
Asphalt 15|15ºC|1000Hz	8.49	14.4	7.14e+4	1019
Asphalt 40|35ºC|1000Hz	1.96	5.72	2.33e+4	582
Asphalt 40|35ºC|550Hz	1.60	4.93	1.99e+4	538

In order to investigate whether the assumption of a rigid bond between asphalt and deck plate overestimates the frequency change, the calculation was repeated using no shear bond between either asphalt layer and the steel deck plate. This is a lower-bound approximation and is summarized in Table 6. Assuming no shear bond, the reduction is still 31.5%.

Table 6 Deck plate subsystem, no shear bond.

Input	E_{zoab} GPa	E_{guss} GPa	EI Nm^2	f_1 Hz
Asphalt 15|15ºC|300Hz	7.22	12.2	6.11e+3	298
Asphalt 40|35ºC|300Hz	1.29	4.21	2.99e+3	209
Asphalt 40|35ºC|200Hz	1.11	3.77	2.85e+3	204

6.2 Subsystem 2: Stiffener, deck plate and asphalt

The second subsystem contains a longitudinal stiffener with a 300 mm wide section of deck plate and asphalt. This is equal to the c.t.c. distance of the stiffeners. Geometry and support conditions are shown in Figure 18.

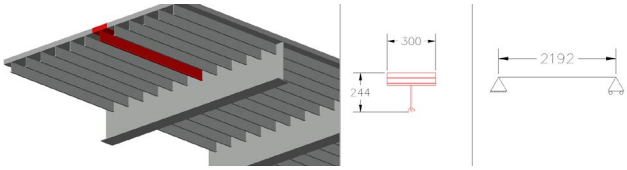

Figure 18 Stiffener and deck plate sub system

Using the same approach as before, the change in first eigenfrequency due to a temperature change is determined, as shown in Table 7. At night the frequency is approximately 73.2 Hz, and during a warm day this reduces to 68.6 Hz. A drop of 6.3%.

Table 7 Stiffener and deck plate sub system

Input	E_{zoab} GPa	E_{guss} Gpa	EI Nm^2	f_1 Hz
Asphalt 15|15ºC|70Hz	5.65	9.60	3.80e+6	73.2
Asphalt 40|35ºC|70Hz	0.74	2.78	3.34e+6	68.6

6.3 Subsystem 3: One full span.

The largest system considered is a single span of the 10-span continuous bridge, as shown in Figure 19.

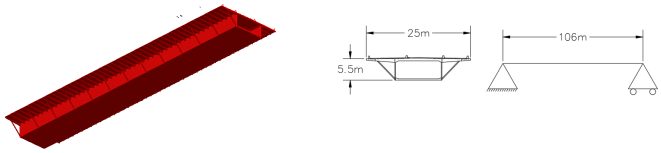

Figure 19 One bridge span subsystem

As shown in Table 8 the influence of asphalt temperature is small. The drop in frequency is smaller than 0.8%. This is based on a homogeneous asphalt temperature change. Section 3 has shown this assumption may not be valid for the entire span, and the influence may thus be smaller.

Table 8 Bridge span

Input	E_{zoab} Gpa	E_{guss} Gpa	EI Nm^2	f_1 Hz
Asphalt 15|15ºC|1.3Hz	2.07	3.87	6.8e+11	1.27
Asphalt 40|35ºC|1.3Hz	0.13	0.73	6.7e+11	1.26

7 CONCLUSIONS

The Haringvlietbrug measurement campaign shows that significant local temperature differences may occur in steel box girder bridges due to local shade. The observed temperature gradients did not fully align with temperature gradients according to the Eurocode and other standards. Global temperature gradients may suffice for the Eurocodes' purpose, namely ULS and SLS design, but compensating for environmental influences in SHM requires a detailed investigation of the temperature distributions.

Using discrete subsystems the influence of temperature-dependent asphalt stiffness has been found to be the largest contributor to changes in local vibration frequencies, outweighing the effects of temperature-induced stress. These results have not yet been verified with vibration measurements, which is part of ongoing research.

The presented research results in this paper may help to improve setups of future SHM-campaigns, by taking into account the following:

- The temperature-dependent asphalt stiffness should be considered when designing SHM systems that use features extracted from local/high-frequency vibrations of the deck plate. Both the local asphalt temperature and the asphalt master curve are of importance.
- The complexity of the observed temperature gradients suggests that common SHM-approaches where only ambient temperature and a limited amount of discrete element temperatures are measured, may not capture the full temperature distribution and the resulting temperature-induced stress. This may significantly limit the ability to account for these effects.
- The complexity of the gradients also suggests that placing enough sensors to capture all possible gradients will not result in practical, cost-effective solutions. Rudimentary 1D-heatflow models using basic inputs such as geometry, solar radiation and inclination, ambient temperature, wind speed and rain are shown to predict the occurring temperature and temperature-gradients in the cantilevered part of the deck. The 1D-approach has also shown that additional information about the air temperature inside the main box-girder seems required to make the 1D-approach capable of accurately describing the behaviour of the deck above the box. Using higher order heat flow models could result in accurate simulation of the temperature distribution in the entire bridge, and therefore parameters such as solar radiation and inclination may be better suited as inputs for learning algorithms, rather than discrete temperature measurements.
- Just before sunrise the amplitude of temperature gradients and the resulting temperature-induced stress are smallest, making this period useful for either SHM-measurements, or for calibrating equipment.

ACKNOWLEDGMENTS

The support of Rijkswaterstaat for supplying access to the Haringvlietbrug and funding of the measurement campaign is greatly acknowledged. In particular we would like to express our gratitude to Jaap van der Heide (Rijkswaterstaat) for his efforts to create this opportunity for the team. The support of Axel Lok (University of Twente) for his assistance in the setup and installation of the vibration monitoring system was of great help to the project. Lastly, Cor Kasbergen and Kumar Anupam (Delft University of Technology) are acknowledged for their assistance and review of the asphalt modelling.

REFERENCES

[1] H. Sohn, *Effects of Environmental and Operational Variability on Structural Health Monitoring*, Phil. Trans. R. Soc. A 365, 539–560, 2017.

[2] E. J. Cross, G. Manson, K. Worden, S. G. Pierce, *Features for damage detection with insensitivity to environmental and operational variations*, Proc. R. Soc. A 468, 4098–4122, 2012.

[3] K. Worden, H. Sohn, C.R. Farrar, *Novelty detection in a changing environment: regression and interpolation approaches*, J. Sound Vib. 258, 741–761, 2002.

[4] Herbert Leaderman. *Elastic and Creep Properties of Filamentous Materials*. Thesis. Massachusetts Institute of Technology, 1941. url: https://dspace.mit.edu/handle/1721.1/45989

[5] Malcolm L. Williams, Robert F. Landel, and John D. Ferry, *The Temperature Dependence of Relaxation Mechanisms in Amorphous Polymers and Other Glass-forming Liquids.*, Journal of the American Chemical Society 1955 77 (14), 3701-3707 DOI: 10.1021/ja01619a008

[6] NEN, NEN-EN 1991-1-5: *Eurocode 1: Belastingen op constructies - Deel 1-5: Algemene belastingen – Thermische belasting.*

[7] NEN, *Nationale bijlage bij NEN-EN 1991-1-5+C1: Eurocode 1: Belastingen op constructies - Deel 1-5: Algemene belastingen - Thermische belasting.*

[8] DIN 1072:1985, Strassen- und Wegbrücken – Lastannahmen

[9] www.sunearthtools.com, *Solar inclination and Azimuth data were obtained for the bridge location at a date of May 30 2020*

[10] www.knmi.nl, *Ambient temperature and solar intensity on a horizontal surface, provided at 10 minute intervals for the Rotterdam station*

[11] ARA, Inc. ERES Consultants Division. *Guide for Mechanistic–Empirical Design of New and Rehabilitated Pavement Structures*. Final Report to the National Cooperative Highway Research Program. NCHRP, Washington, D.C., March 2004.